

Electrical conductivity of amorphous silicon doped with rare-earth elements

J. H. Castilho, I. Chambouleyron,* F. C. Marques, C. Rettori, and F. Alvarez

Instituto de Física, Universidade Estadual de Campinas, P.O. Box 6165, Campinas, São Paulo, 13081 Brazil

(Received 17 December 1990)

This work reports on the electrical properties of *a*-Si samples doped with elements of the lanthanide series. A detailed study of gadolinium-doped *a*-Si is presented. It has been found that the introduction of rare-earth elements into the amorphous-silicon network produces large changes in the conductivity. An analysis of the experimental conductivity as a function of temperature and rare-earth content, together with the optical and electron-spin-resonance data, leads us to suggest that rare-earth-acceptor-like states located in the lower half of the pseudogap may be responsible for the measured properties.

INTRODUCTION

Rare-earth (*R*) elements are of interest because their incomplete *4f* subshells give physical properties that are useful, such as stimulated emission, when incorporated into various crystalline hosts. Relatively little work has been done on the incorporation of rare-earth elements into covalent semiconductors, such as silicon and germanium, because of their rather low solubilities. Mandelkorn *et al.*¹ prepared Gd-doped (*p*-type) silicon ingots in the 10–20- Ω cm range, but apparently only a small percentage of the impurities undergo room-temperature ionization, an indication of a rather large ionization energy or a more complex impurity-atom–lattice interaction. These authors concluded that gadolinium, as well as other rare-earth elements, exhibits valence behavior similar to elements in group III of the Periodic Table. Antonenko *et al.*² grew Si single crystals by the Czochralski method adding rare-earth elements to the melt, and found that the rare-earth elements Gd and Sm are passive impurities, acting as sinks for one component of the Frenkel pairs or as an annihilation center. Gibbons *et al.*³ bombarded silicon crystals with thulium and neodymium ions and found deep-donor-like centers, with activation energies between 0.25 and 0.5 eV, most probably produced by rare-earth impurities in interstitial positions. Sclar⁴ explored the applicability of thulium and ytterbium as impurities in silicon extrinsic infrared detectors. These dopants were found to behave as deep donors in the Si lattice but were of little use because of the low solubilities obtained. The diffusion of rare-earth elements in crystalline germanium was studied by Gusev *et al.*⁵ (Ce, Nd, Tb, Lu, Yb) but their electrical activity is not reported. The magnetoresistance of germanium doped with neodymium and europium has been reported by Lashkarev *et al.*⁶ However, no references to the nature of ionization energies of these impurities are given.

The existing literature, thus, exhibits some degree of uncertainty on the doping properties of rare-earth elements in covalent semiconductors. The difficulty derives partly from their low solubility in the crystalline lattice which promotes agglomerates hindering the doping ac-

tivity of isolated elements. The problems related to the low solubility of rare-earth atoms in crystalline silicon and germanium lattices may be partially overcome in amorphous networks, in which the lack of long-range order permits the structure to accommodate atoms of greatly different sizes. Moreover, Spear and LeComber⁷ established that the doping properties of atoms of columns III and V of the Periodic Table are, in tetrahedrally bonded amorphous semiconductors, similar to those found in the crystalline semiconductor parents.

With these ideas in mind, we undertook a study of the doping properties of rare-earth elements in *a*-Si networks. This work reports on the electrical properties of *a*-Si samples doped with elements of the lanthanide series. A detailed study of gadolinium-doped *a*-Si was made. It has been found that the introduction of rare-earth elements into an amorphous Si network produces large changes in the conductivity. The analysis of the experimental data leads us to suggest that rare-earth-acceptor-like states localized in the lower half of the pseudogap may be responsible for these changes in the conductivity.

EXPERIMENT

Amorphous silicon–rare-earth films (*a*-Si_{1-x}R_x) were deposited by rf sputtering a compound target in an Ar atmosphere. The target, a high-purity *c*-Si disk, was covered at random by small pieces of rare-earth elements. The nominal rare-earth concentration was always estimated from the rare-earth target coverage and the sputtering yield for each element. Sample thicknesses (typically 2–4 μ m) were determined from the optical interference fringes appearing in the ir transmission spectra. In some cases, however, large optical absorption resulted from the doping and so the sample thickness had to be estimated from the deposition rate. Aluminum electrodes were vacuum evaporated onto the samples. Electrical-conductivity measurements were performed in the 90–420-K temperature range. More detailed information on sample preparation and texture, optical properties, spin densities, and other experimental conditions are given in Ref. 8.

RESULTS AND DISCUSSION

Figure 1 shows the temperature dependence of the conductivity of *a*-Si films having ~ 0.1 at.% (nominal concentration) of several rare-earth elements in the amorphous network. The elements being reported are lanthanum, praseodymium, neodymium, erbium, and lutetium. Similar results are obtained for gadolinium doping. In Fig. 1 the conductivity of an undoped *a*-Si film has been plotted for comparison. It may be seen in the figure that, for all the rare-earth elements used a large conductivity drop results from the rare-earth doping process. Let us note that the results can be well fitted by⁹

$$\sigma(T) = \sigma_h \exp[-(T_0/T)^{1/4}], \quad (1)$$

where¹⁰

$$T_0 = 16\alpha^3 / N(E_F)k_B, \quad (2)$$

in which $N(E_F)$, α , and k_B designate, respectively, the density of states at E_F , the decay constant of the localized-state wave function, and the Boltzmann constant.

In all cases, a straight line is obtained, suggesting a variable-range-hopping conduction mechanism⁹ for the electrical conductivity in these films. For the sake of clarity only the low-temperature side of the data have been plotted. A well-defined $T^{-1/4}$ straight-line plot allows us to calculate the value of T_0 . The results are shown in Table I. They indicate an increased T_0 , as compared with the value obtained in undoped *a*-Si, consistent with a reduced density of states at the Fermi level.

The differences in the absolute conductivity of the doped samples shown in Fig. 1 arise, within experimental

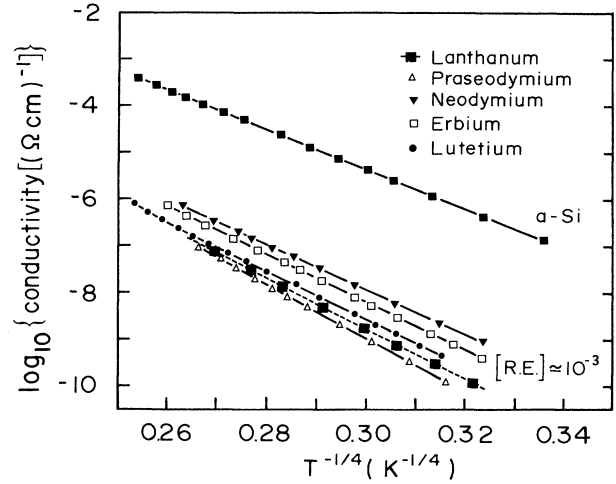


FIG. 1. Logarithm of the conductivity vs $T^{-1/4}$ for rare-earth-doped *a*-Si samples. The nominal impurity concentration, as determined by the sputtering yield of the elements and the target coverage, is of $\sim 10^{-1}$ at.% in all cases. The variation of the conductivity of an undoped *a*-Si sample prepared under conditions identical to those of the rare-earth-doped samples is also shown.

errors, from uncertainty in the sputtering yield, rare-earth target coverage, and sample thickness. Consequently, they should not be attributed to different rare-earth doping efficiencies or impurity-level energies.

Figure 2 shows the logarithm of the conductivity of Gd-doped *a*-Si films versus $T^{-1/4}$ for samples with vari-

TABLE I. Characteristics of $a\text{-Si}_{1-x}\text{:R}_x$ samples.

Rare-earth content (x)	Optical gap (eV)	σ_{RT} [($\Omega\text{ cm}$) ⁻¹]	D^0 (spin/cm ³)	T_0 (K) (10 ⁶)
<i>a</i> -Si 0.0000	1.20±0.02	1.3×10^{-3}	2.1×10^{18}	84
Gd 0.0005		6.9×10^{-7}	3.5×10^{17}	
0.0010	1.20±0.03	1.6×10^{-6}	1.3×10^{17}	
0.0023	1.10±0.02		3.1×10^{16}	
0.0060	0.63±0.02	1.9×10^{-4}		58
0.0100	0.11±0.02	1.8×10^{-3}		22
0.0160		7.1×10^{-3}		15
0.0300		3.0×10^{-1}		0.14
La 0.0010		1.2×10^{-5}	9.0×10^{17}	230
Pr 0.0010		3.9×10^{-6}	6.0×10^{17}	307
Nd 0.0010		8.3×10^{-6}	3.0×10^{17}	154
Er 0.0010		7.3×10^{-6}	5.0×10^{17}	188
Lu 0.0010		3.1×10^{-6}	1.0×10^{17}	188
0.0100		1.3×10^{-1}		0.81

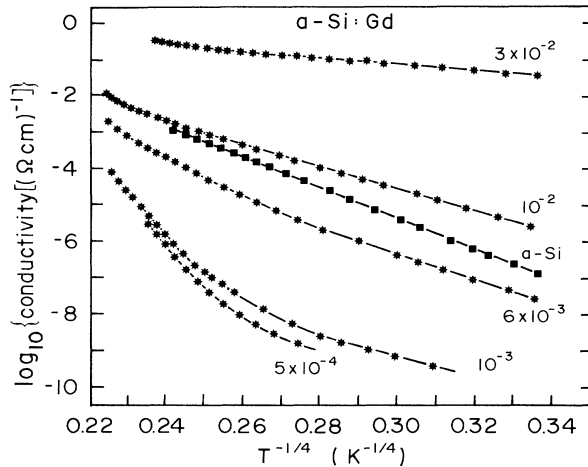


FIG. 2. Logarithm of the conductivity vs $T^{-1/4}$ for gadolinium-doped a -Si samples. The nominal impurity concentration, as determined by the sputtering yield of Gd and the target coverage, varies between 5×10^{-4} and 3×10^{-2} . It can be clearly seen that the conductivity experiences a large decrease at small impurity concentrations but tends toward larger values at higher dopant content.

ous impurity concentrations. As for the other rare-earth elements, the addition of minute amounts of Gd decreases the low-temperature conductivity of a -Si films by a large factor. This is an indication that the density of states at the Fermi level decreases considerably. Note that, contrary to the case of the rare-earth elements of Fig. 1, the Gd concentration curve for $x \cong 10^{-3}$ does not display a clear $T^{-1/4}$ dependence. This difference may be due to a poor estimate of the Gd sputtering yield, to an error in the determination of the target coverage, or to a different active doping efficiency. The abrupt conductivity decrease with light rare-earth doping is simultaneous with the reduction of the electron-spin density, shown in Table I. The disappearance of the dangling-bond ESR signal as a consequence of the increase in the rare-earth concentration is also indicative of a shift of the Fermi level away from the energy region of the dangling bond D^0 , which normally pins the Fermi level in the pseudogap of undoped a -Si samples.

The present experimental conditions give a minimum conductivity for a concentration of $\sim 5 \times 10^{-4}$ at.% Gd, but it is not meant here that at this concentration the absolute conductivity minimum is obtained. As the Gd nominal concentration increases above this value, the conductivity of the samples increases, tending toward a classical variable-range-hopping conduction behavior. The trend indicates that Gd concentrations higher than the maximum ($\cong 3$ at.%) investigated in this work would eventually lead to a metalliclike conductivity. In Fig. 2, the conductivity of an undoped a -Si film prepared under identical conditions is shown for comparison.

Figure 3 shows the high-temperature behavior of the conductivity for lightly Gd doped a -Si samples. The nominal Gd concentrations are 5×10^{-4} and 10^{-3} at.%. In this figure, the logarithm of the conductivity is plotted

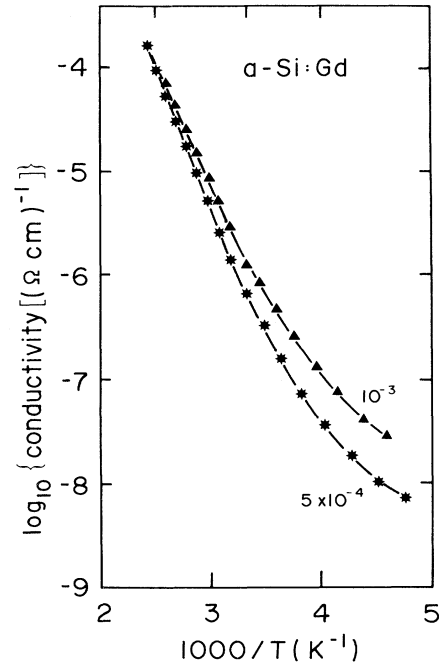


FIG. 3. Logarithm of the conductivity vs inverse temperature for gadolinium-doped a -Si samples with low impurity concentration. Above room temperature the conductivity is seen to display an activated-type behavior with activation energies of nearly 0.5 eV.

versus the inverse temperature. It is clear from Fig. 3 that the contribution of an activated-like conductivity path, i.e., $\sigma = \sigma_0 \exp[-(E_a/k_B T)]$, becomes predominant above room temperature. σ_0 , of the order 10^3 ($\Omega \text{ cm})^{-1}$, and activation energies of around 0.5 eV, are obtained from the data.

Figure 4 displays the room-temperature conductivity of Gd-doped silicon samples as a function of Gd nominal concentration. The data pointed to by an arrow indicates samples in which the thickness has been estimated from the deposition rate. The strong dependence of the room-temperature conductivity on the Gd concentration is indicative of the active role played by these impurities in the amorphous network. The behavior shown in Fig. 4 is similar to the one displayed by the conductivity of Au-doped a -Si samples, an impurity known to produce an acceptorlike level in the lower half of the a -Si pseudogap.¹¹

The present results give evidence of the active nature of the rare-earth doping process in a -Si films. In that sense, and particularly with the results concerning Gd-doped samples, our data confirm the findings of Mandelkorn *et al.*,¹ who succeeded in producing p -type crystalline silicon ingots adding Gd to the melt. The rare-earth valence is normally 3+, but this fact does not explain by itself why they would create an acceptorlike state in a tetrahedrally bonded semiconductor. In a previous publication,¹² the following explanation was suggested. For a substitutional rare-earth atom the local tetrahedral field may split the $5d$ rare-earth orbital, leading to a triplet ground state (t_2), which could hybridize with the $6s$

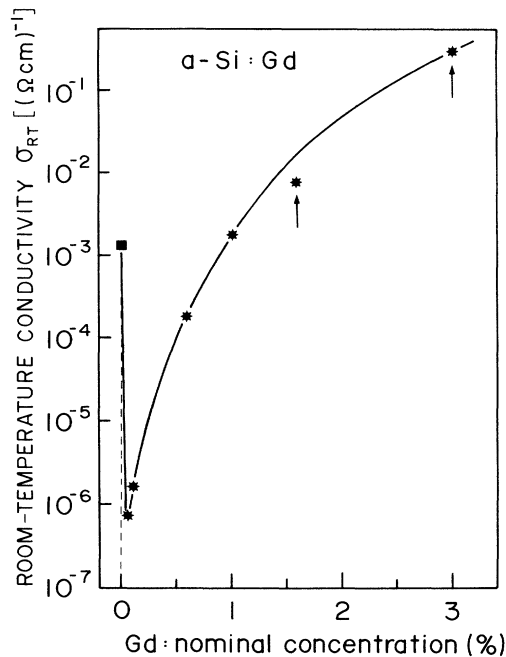


FIG. 4. Room-temperature conductivity of Gd-doped *a*-Si samples as a function of gadolinium concentration. The large conductivity variations result from the displacement of the Fermi level within the pseudogap. The experimental points indicated by the arrows correspond to samples having a large absorption coefficient. The thickness of these samples was estimated from the deposition rate.

rare-earth orbital forming four sd^3 bonds, three of which may be occupied by the rare-earth valence electrons, the fourth being unoccupied. The four rare-earth bonds formed in this way can be saturated by nearby Si atoms and an extra electron taken from neutral dangling bonds or valence-band states. This picture is illustrated in Fig. 5. At low Gd concentrations, the Fermi level is shifted downwards toward a region of smaller density of states. This shift accounts for the decrease of the ESR signal, the conductivity, and the appearance of an activated type of conduction at high temperatures (holes in valence-band extended states). A further increase in dopant content may create a parallel conduction path through the localized impurity levels, giving a $T^{-1/4}$ -type conductivity behavior. An increasing impurity content would lead, eventually, to an impurity band. The conductivity behavior of *a*-Si films as a function of dopant content and temperature, shown in Fig. 2, the optical properties, and the ESR signal decrease with increasing Gd concentration, are consistent with this picture.

Figure 6 shows T_0 [see Eq. (2)] versus Gd concentration for Gd-doped *a*-Si samples having the conductivity dominated by impurity states. An important decrease of T_0 with increasing impurity content is seen in Fig. 6. This decay probably arises from the decay length (α^{-1}) of the localized wave function of the hopping electrons around E_F , which is expected to increase with increasing impurity content, and from a larger density of states

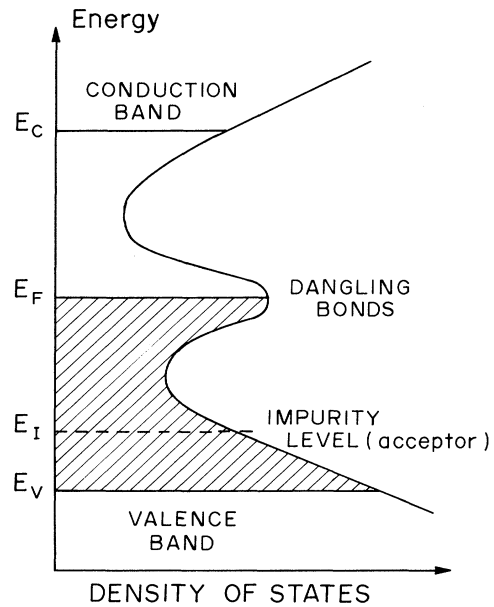


FIG. 5. Sketch of the density of states in the pseudogap of *a*-Si vs energy. An acceptor level in the lower half of the pseudogap produced by rare-earth impurities may explain the conductivity variations and the ESR data of rare-earth-doped *a*-Si samples.

$N(E_F)$ at the Fermi energy coming from an increased impurity content.

It is interesting to speculate on the degree of localization of the hopping-electron wave function. Let us assume that, for high Gd concentration, the main contribution to $N(E_F)$ comes from the rare earth, i.e.,

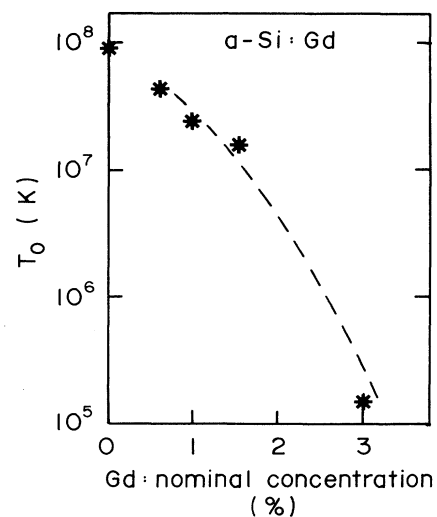


FIG. 6. T_0 , as determined from Eq. (1), vs Gd nominal concentration, for Gd-doped *a*-Si samples in which the conductivity is dominated by impurity states.

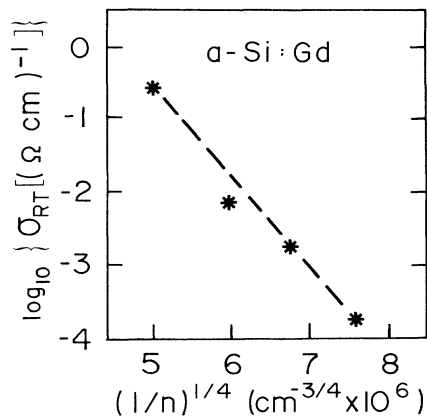


FIG. 7. Logarithm of the room-temperature electrical conductivity σ_{RT} vs $(1/n)^{1/4}$, for Gd-doped *a*-Si films in which the conductivity is dominated by impurity states. The crystalline Si atomic concentration ($5 \times 10^{22} \text{ cm}^{-3}$) has been used in the calculations.

$N(E_F) \cong bn$, where b^{-1} corresponds to the width of the impurity-localized-state bump and n is the active-defect density produced by the rare earth. We may assume, as for other dopants, that the active doping efficiency of rare-earth elements in *a*-Si is a small number, say $n/N_R \cong 10^{-2}$. Under these assumptions, the variable-range-hopping conductivity equation reads

$$\sigma = \sigma_h \exp[-(n_0/n)^{1/4}], \quad \text{with } n_0 = 16\alpha^3/bk_B T. \quad (3)$$

Figure 7 shows the logarithm of the room-temperature conductivity versus $n^{-1/4}$ for Gd-doped *a*-Si samples ($0.006 \leq x \leq 0.03$). As expected from Eq. (3), an exponential dependence of σ_R on $n^{-1/4}$ is obtained. Assuming an energy width of the order of 0.25 eV for the impurity levels, a decay length $1/\alpha \cong 5 \text{ \AA}$ is obtained with the present data, suggesting that the rare-earth states are rather localized in *a*-Si.

CONCLUSIONS

This paper addresses the problem of the doping activity of rare-earth elements in amorphous silicon networks. Conductivity measurements on samples prepared with various concentrations of different elements of the lanthanide series show that rare-earth induce large changes in the electrical properties of the amorphous films. The experimental dependence of the conductivity on temperature and rare-earth concentration, and the optical and ESR data, are consistent with a model postulating the existence of a rare-earth-acceptorlike level localized in the lower half of the pseudogap. The origin of such a state in terms of hybridized rare-earth orbitals was also discussed.

ACKNOWLEDGMENTS

The authors are indebted to Professor G. Barberis for fruitful discussions. The help of M. I. Romeiro is also acknowledged. This research was partially supported by the Conselho Nacional de Desenvolvimento Científico e Tecnológico (CNPq), and the Fundação de Amparo à Pesquisa do Estado de São Paulo (FAPESP).

*To whom correspondence should be addressed.

¹J. Mandelkorn, L. Schwartz, J. Broder, H. Kautz, and R. Ullman, *J. Appl. Phys.* **35**, 2258 (1964).

²R. Antonenko, Yu. Karpov, V. Shakhovtsov, V. Shindich, L. Shpinar, and I. Yaskovets, *Fiz. Tekh. Poluprovodn.* **12**, 1853 (1978) [*Sov. Phys.—Semicond.* **12**, 1011 (1978)].

³J. Gibbons, J. Moll, and N. Meyer, *Nucl. Instrum. Methods* **38**, 165 (1965).

⁴N. Sclar, *Infrared Physics* **17**, 71 (1977).

⁵I. Gusev, L. Molkanov, and A. Murin, *Fiz. Tverd. Tela. (Leningrad)* **6**, 1256 (1964) [*Sov. Phys.—Solid State* **6**, 980 (1964)].

⁶G. Lashkarev, A. Dmitriev, G. Sukach, and V. Shershel, *Fiz.*

Tekh. Poluprovodn. **5**, 2075 (1972) [*Sov. Phys.—Semicond.* **5**, 1808 (1972)].

⁷W. Spear and P. LeComber, *Solid State Commun.* **17**, 1193 (1975); *Philos. Mag.* **33**, 935 (1976).

⁸J. Castilho, G. Barberis, C. Rettori, F. C. Marques, I. Chambouleyron, and F. Alvarez, *Phys. Rev. B* **39**, 8398 (1989).

⁹N. F. Mott, *Philos. Mag.* **19**, 835 (1969).

¹⁰V. Ambegaokar, B. Halperin, and J. Singer, *Phys. Rev. B* **4**, 2612 (1972).

¹¹N. Kishimoto and K. Morigaki, *J. Phys. Soc. Jpn.* **46**, 846 (1979).

¹²J. Castilho, F. C. Marques, G. Barberis, C. Rettori, F. Alvarez, and I. Chambouleyron, *Phys. Rev. B* **39**, 2860 (1989).